intend to study this effect and other nonsymmetrical junctions in a future publication.

References

[1] J. B. Davies, "An analysis of the m-port symmetrical H-plane waveguide junction with central ferrite post," *IRE Trans. Microwave Theory Tech. (1962 Symposium Issue)*, vol. MTT-10, pp. 596–604, Nov. 1962.

[2] L. E. Davis and J. B. Castillo, Jr., "Computer-aided design of 3-port waveguide circulators," R&D Tech. Rep. ECOM-0491-F, Oct. 1968.

[3] J. B. Castillo, Jr., and L. E. Davis, "Computer-aided design of 3-port waveguide junction circulators," *IEEE Trans. Microwave Theory Tech.*, vol. MTT-18, pp. 25–34, Jan. 1970.

[4] L. Lewin and E. Nielsen, "On the inadequacy of discrete mode-matching techniques in some waveguide discontinuity problems," *IEEE Trans. Microwave Theory Tech.*, vol. MTT-18, pp. 364–372, July 1970.

[5] L. Lewin, "On the restricted validity of point-matching techniques," *IEEE Trans. Microwave Theory Tech. (1970 Symposium Issue)*, vol. MTT-18, pp. 1041–1047, Dec. 1970.

[6] W. W. Siekanowicz and W. A. Schilling, "A new type of latching switchable ferrite junction circulator," *IEEE Trans. Microwave Theory Tech.*, vol. MTT-16, pp. 177–183, Mar. 1968.

[7] H. Y. Yee and N. F. Audeh, "Uniform waveguides with arbitrary cross-section considered by the point-matching method," *IEEE Trans. Microwave Theory Tech. (1965 Symposium Issue)*, vol. MTT-13, pp. 847–851, Nov. 1965.

[8] J. A. Fuller and N. F. Audeh, "The point-matching solution of uniform nonsymmetric waveguides," *IEEE Trans. Microwave Theory Tech.* (Corresp.), vol. MTT-17, pp. 114–115, Feb. 1969.

[9] R. H. T. Bates, "The point-matching method for interior and exterior two-dimensional boundary value problems," *IEEE Trans. Microwave Theory Tech.* (Corresp.), vol. MTT-15, pp. 185–187, Mar. 1967.

[10] J. B. Castillo and L. E. Davis, "A higher order approximation for waveguide circulators," *IEEE Trans. Microwave Theory Tech.* (Short Paper), vol. MTT-20, pp. 410–412, June 1972.

Equivalent Circuit for Partially Dielectric-Filled Rectangular-Waveguide Junctions

C. T. M. CHANG

Abstract—**The problem of electromagnetic-wave propagation in junctions between two symmetrically, partially dielectric-filled waveguides was investigated, and the solution is presented in the form of a two-port equivalent circuit. This equivalent circuit includes an ideal 1:1 transformer, which is connected to transmission lines with impedances equal to those of the two waveguides, in cascade with a T network. Elements of the T network and the characteristic wave impedances of these partially dielectric-filled waveguides have been studied, and the results are presented in graphs for different dielectric constants, slab thicknesses, and operating frequencies.**

I. Introduction

IN RECENT YEARS there has been growing interest in waveguide sytems containing sections of partially dielectric-filled rectangular waveguides. Considerable literature has been devoted to the study of the different characteristics of partially dielectric-filled waveguides [1]–[10] and their applications to various microwave devices [11]–[15]. In many of these applications, the partially dielectric-filled waveguides are fed by empty waveguides and are sometimes terminated into another empty waveguide. Therefore, it is important that the characteristics of the junctions between the empty and partially dielectric-filled waveguide be studied so that some impedance-matching techniques [16] may be developed to minimize reflections at different locations along the waveguide system.

Earlier, several attempts [4], [17]–[19] were made to obtain the equivalent circuits for a number of empty to partially dielectric-filled rectangular-waveguide junctions employing various modified schemes of variational methods developed by Schwinger [20]. However, only a few crude calculations using simplified equivalent circuits were presented, and they were justified by comparing their results to reflection measurements. The reflection from a waveguide junction is caused by the change of the characteristic wave impedances across the junction, as well as the junction reactances, which are due to the stored energy in the nonpropagating modes at the junction. The reflections given in the examples in these earlier works were caused primarily by the former. Therefore, it becomes difficult to extract the small effect due to junction reactances from the experimental measurements and make an accurate comparison.

In the present work we report an investigation of dielectric-filled waveguide junctions in six different arrangements. It is found that despite their differences in geometries, they can all be represented by the equivalent circuit of Fig. 1(g). The effects of dielectric constants, thickness of dielectric slabs, and operating frequencies on various equivalent circuit parameters were studied and compared so that some general properties of these junctions could be understood.

Since this work is stimulated by the development of a microwave discharge chamber [21] that is partially dielectric filled and is operating in the dominant transverse electric (TE) mode,[1] present investigation is limited to junctions in-

Manuscript received September 7, 1972; revised January 26, 1973. This work was performed under the auspices of the U. S. Atomic Energy Commission.

The author is with the Argonne National Laboratory, Argonne, Ill. 60439.

[1] It should be noted that modes propagating inside a partially dielectric-filled waveguide are, in general, a mixture of regular TE and TM modes of the rectangular waveguide (see [1]).

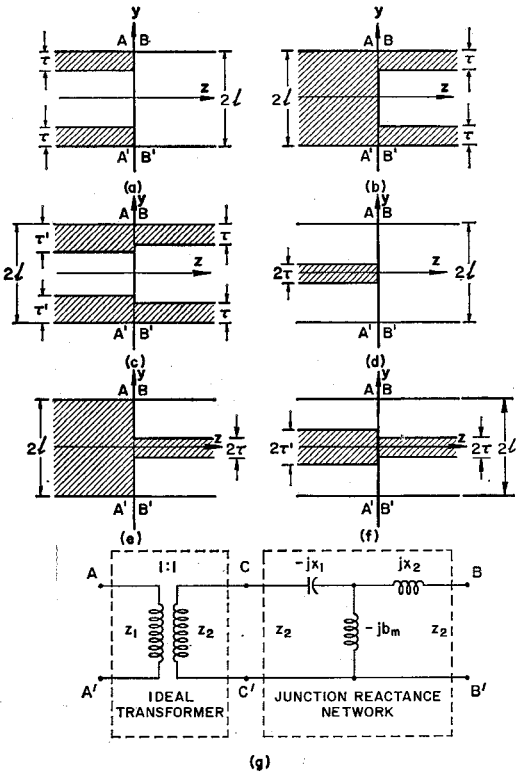

Fig. 1. Geometries (shown in top view) and the equivalent circuit of the partially dielectric-filled rectangular-waveguide junctions. (a) Empty to side-slab-filled waveguide junction. (b) Completely filled to side-slab-filled waveguide junction. (c) Junction between two side-slab-filled waveguides. (d) Empty to center-slab-filled waveguide junction. (e) Completely filled to center-slab-filled waveguide junction. (f) Junction between two center-slab-filled waveguides. (g) Equivalent circuit for junctions shown in (a)–(f).

volving TE modes. In the next few sections, the junction between an empty waveguide and a side-slab-filled waveguide [Fig. 1(a)] is chosen to describe the method by which the problem is attacked. Some of the important relations of TE_{0m} modes in side-slab-filled waveguides are presented in Section II for reference. In Section III a unit field is incident on the junction, expanded into two complete sets of orthogonal modes, and matched at the junction. With the aid of a matrix inversion, the complex amplitudes of the modal expansion are obtained and the field problem is thus completely solved. In many instances, only the knowledge of the transmitting and reflecting coefficients of the propagating modes is required. It is convenient to represent a junction by a microwave network so that its effect may be separated from those of the input and output circuits and may be studied by employing a minimum number of parameters. This is done in Section IV. With the restriction that only one mode is allowed to propagate in each waveguide, the junction is adequately represented by a two-port network. This is further divided into two cascade networks to separate the effects due to the discontinuity in the characteristic impedance and the junction reactances. Numerical computations and results of the investigation are presented in Section V for the junction of Fig. 1(a) and are extended to the junctions of Fig. 1(b)–(f) in Section VII. Several experimental measurements are also presented in Section VI for comparison.

II. The TE Modes in Partially Dielectric-Filled Waveguides

For TE_{0m} modes the electric field is

$$E_x = A_m F_m(y) e^{\mp j h_m z} \tag{1}$$

and the magnetic fields are

$$H_y = \pm E_x / Z_m \tag{2}$$

and

$$H_z = \pm j \frac{A_m}{h_m Z_m} \frac{dF_m(y)}{dy} e^{\mp j h_m z} \tag{3}$$

where the upper and lower signs apply to waves propagating to the right and to the left, respectively, h_m is the propagation constant of the mth mode, and the field distribution with y-symmetry[2] is given by

$$F_m(y) = \frac{1}{\sqrt{2\Lambda_m^{(1)}}} \cdot \begin{cases} \sin \alpha_m \tau \cos \gamma_m y, & 0 < |y| < l - \tau \\ \cos \gamma_m (l - \tau) \sin \alpha_m (l - |y|), & l - \tau < |y| < l \end{cases} \tag{4}$$

$$m = 1, 3, \cdots$$

and

$$Z_m = k_0 \eta_0 / h_m \tag{5}$$

where

$$\eta_0 = (\mu_0/\epsilon_0)^{1/2} \qquad k_0 = (2\pi f/c). \tag{6}$$

Here, μ_0, ϵ_0, and c are the permeability, the permittivity, and the speed of light in free space, respectively, f is the operating frequency, and α_m and γ_m are the separation constants in y. The matching of fields across the dielectric interfaces demands that

$$\gamma_m \tan \gamma_m (l - \tau) = \alpha_m \cot \alpha_m \tau. \tag{7}$$

Also, α_m and γ_m satisfy the following relations:

$$\alpha_m^2 - \gamma_m^2 = (\epsilon_r - 1) k_0^2 \tag{8}$$

and

$$\alpha_m^2 - \epsilon_r \gamma_m^2 = (\epsilon_r - 1) h_m^2. \tag{9}$$

The normalization constant $\Lambda_m^{(1)}$ is obtained from the orthogonal relation

$$\int_{-l}^{l} F_m(y) F_{m'}(y)\, dy = \delta_{mm'} \tag{10}$$

where $\delta_{mm'}$ is the Kronecker delta function.

III. The Field Problem of a Waveguide Junction

As shown in Fig. 1(a), the junction under consideration is chosen to be a junction between a partially dielectric-filled waveguide and an empty waveguide. These two waveguides meet at $z = 0$ and are extended to $-\infty$ and $+\infty$, respectively.

[2] Modes with even m are antisymmetric. They do not enter into the present analysis.

With an electromagnetic wave incident from $z=-\infty$, the field is represented by

$$E_x = f_1(y)e^{-jh_1z} + \sum_{m=1,3,\cdots}^{\infty}{}' a_m f_m(y)e^{jh_mz} \tag{11}$$

and

$$H_y = \frac{f_1(y)}{Z_1}e^{-jh_1z} - \sum_{m=1,3,\cdots}^{\infty}{}' \frac{a_m}{Z_m} f_m(y)e^{jh_mz} \tag{12}$$

for $z<0$, where $f_m(y)=F_m(y)$, and

$$E_x = \sum_{n=1,3,\cdots}^{\infty}{}' a_n' g_n(y)e^{-jh_n'z} \tag{13}$$

and

$$H_y = \sum_{n=1,3,\cdots}^{\infty}{}' \frac{a_n'}{Z_n'} g_n(y)e^{-jh_n'z} \tag{14}$$

for $z>0$, where the incident field is assumed to be unity; a_n' and h_n' are amplitudes and propagation constants of the TE_{0n} mode in a rectangular waveguide: $Z_n'=k_0\eta_0/h_n'$, and

$$g_n(y) = \frac{1}{\sqrt{l}}\cos\left[(n-\tfrac{1}{2})\frac{\pi y}{l}\right]. \tag{15}$$

The primes on the summations represent the sums over odd indexes only. The even (TE) modes are not excited due to the y-symmetry of the junction.

By matching E_x and H_y at $z=0$, after the proper application of orthogonal relationships, one obtains

$$1 - a_1 = \sum_{n=1,3,\cdots}^{\infty}{}' a_n' p_{1n} \tag{16}$$

$$\frac{1-a_1}{Z_1} = \sum_{n=1,3,\cdots}^{\infty}{}' \frac{a_n'}{Z_n'} p_{1n} \tag{17}$$

$$a_m = \sum_{n=1,3,\cdots}^{\infty}{}' a_n' p_{mn}, \qquad \text{for } m = 3, 5, 7, \cdots \tag{18}$$

$$-\frac{a_m}{Z_m} = \sum_{n=1,3,\cdots}^{\infty}{}' \frac{a_n'}{Z_n'} p_{mn}, \qquad \text{for } m = 3, 5, 7, \cdots \tag{19}$$

where

$$p_{mn} = \int_{-l}^{l} f_m(y)g_n(y)\,dy. \tag{20}$$

Equations (16)–(19) represent two infinite sets of linear equations with two infinite sets of variables. They may be rewritten in matrix form. The two infinite sets of variables a_m and a_m' may be obtained from matrix inversion. However, (16)–(19) can be simplified by eliminating a_m and can be combined into

$$\sum_{n=1,3,\cdots}^{\infty}{}' \frac{1}{2}\left(1+\frac{Z_m}{Z_n'}\right)p_{mn}a_n' = \delta_{1m}. \tag{21}$$

Thus a_n' may be obtained from (21) by inverting the matrix of infinite order (versus 2×infinite order for the previous case). One can also obtain a_m from

$$a_m = \sum_{n=1,3,\cdots}^{\infty}{}' \frac{1}{2}\left(1-\frac{Z_m}{Z_n'}\right)p_{mn}a_n'. \tag{22}$$

IV. The Equivalent Circuit Representation

Following the previous discussion, the field problem is now converted into a circuit representation in the form of Fig. 1(g). Since the characteristic impedances Z_1 and Z_2 of the two waveguides are known, the scattering matrix of the ideal junction (represented by the ideal 1:1 transformer between AA' and CC') is obtained from

$$\begin{aligned} S_{11}^{(i)} &= R_1 = \frac{Z_2-Z_1}{Z_2+Z_1} = -S_{22}^{(i)} \\ S_{12}^{(i)} &= T_{12} = \frac{2Z_1}{Z_1+Z_2} \\ S_{21}^{(i)} &= T_{21} = \frac{2Z_2}{Z_1+Z_2}. \end{aligned} \tag{23}$$

With the aid of (23), the incident fields u_1 and u_2 and the reflected fields v_1 and v_2 at the terminals CC' and BB' of the junction-reactance network (the T network) in Fig. 1(g) are obtained from the following simple transformation:

$$\begin{aligned} v_1^{(1)} &= (a_1 - R_1)/T_{12} \\ u_1^{(1)} &= T_{21} - R_1 v_1^{(1)} \\ u_2^{(1)} &= 0 \\ v_2^{(1)} &= a_1' \end{aligned} \tag{24}$$

where a_1 and a_1' are the reflected and transmitted coefficients of the waveguide system, respectively.

By definition, the scattering coefficients of the junction-reactance network satisfy

$$\begin{aligned} v_1 &= S_{11}u_1 + S_{12}u_2 \\ v_2 &= S_{21}u_1 + S_{22}u_2. \end{aligned} \tag{25}$$

To specify the junction-reactance network completely, the field problem must be repeated with a unit electric field incident from $z=\infty$. The fields at terminal CC' and BB' are again related to the new a_1' (reflection coefficient) and a_1 (transmission coefficient) by

$$\begin{aligned} v_1^{(2)} &= \alpha_1/T_{12} \\ u_1^{(2)} &= -v_1^{(2)}R_1 \\ u_2^{(2)} &= 1 \\ v_2^{(2)} &= \alpha_1'. \end{aligned} \tag{26}$$

Superscripts 1 and 2 are added to u_i and v_i, where $i=1, 2$, in (24) and (26) to indicate whether the u_i and v_i are calculated from fields incident from $z=-\infty$ and $z=+\infty$, respectively. Hence, the scattering coefficients of the junction-reactance network can be solved from (25). Note that 1) since the junction-reactance network is reciprocal, an independent check is automatically provided from the relation $S_{12}\equiv S_{21}$; 2) since the relative positions of the two cascade networks are arbitrarily chosen, identical results can be obtained by inter-

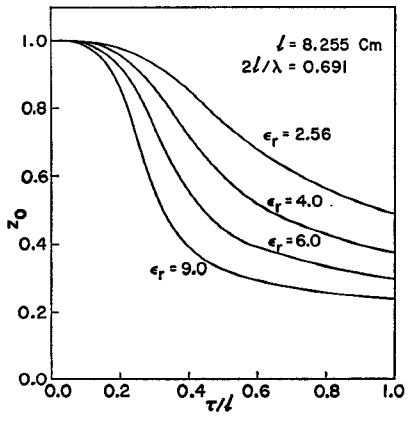

Fig. 2. Normalized characteristic wave impedance z_0 of the side-slab-filled waveguides [the partially filled ones shown in Fig. 1(a)–(c)] versus normalized slab thickness τ/l for different dielectrics.

changing the relative positions; 3) since the field of the TE_{01} mode is no longer purely a sine wave, the equivalent voltage and current are defined to be the sum of the incidence and reflected E_x and the difference of the incidence and reflected H_y of the dominant mode at each point along the waveguide system, respectively.

The scattering-matrix representation is further converted into a T network. The conversions are [22]

$$Z_{S1}/Z_2 = (1 + S_{11} - S_{22} - S_{11}S_{22} + S_{12}^2 - 2S_{12}^2)/D$$
$$Z_{S2}/Z_2 = (1 - S_{11} + S_{22} - S_{11}S_{22} + S_{12}^2 - 2S_{12}^2)/D$$
$$Y_m Z_2 = D/(2S_{12}) \qquad (27)$$

where $D = 1 - S_{11} - S_{22} + S_{11}S_{22} - S_{12}^2$ and Z_1 and Z_2 are the charactristic wave impedances of the partially dielectric-filled and empty waveguides, respectively.

V. Numerical Computations and Results

The success of our calculation depends on the ability to approximate the infinite matrix $\bar{\bar{C}}_{mn}[\equiv \frac{1}{2}(1+(Z_m/Z_n'))p_{mn}]$ given in (21). Since the higher order modes generated at the junction are expected to vanish for large m and n, it is suggested that the infinite matrix may be truncated and substituted by an Nth-order matrix in the actual computation. The accuracies of the first few a_n' will then depend on whether sufficient terms are included in a given approximation. Using the completeness relation

$$\sum_{n=1,3,\cdots}^{\infty}{}' p_{mn}^2 = 1, \qquad \text{for } m = 1, 3, 5, \cdots \qquad (28)$$

as a gauge, the N-term approximation can be qualitatively measured.

Due to the lack of an analytical method for estimating errors in the above approximation, the accuracies in a given calculation are established quantitatively by comparing the junction-network parameters obtained from the N-term and $(N+1)$-term approximations. The separation constants α_m and γ_m (which may be either real or imaginary) were calculated by locating the intersects of (7) and (8) for a given frequency using Descartes' rule of signs.

All calculations were performed in double-precision arithmetic on IBM 360. The matrix-inversion subroutine is carried

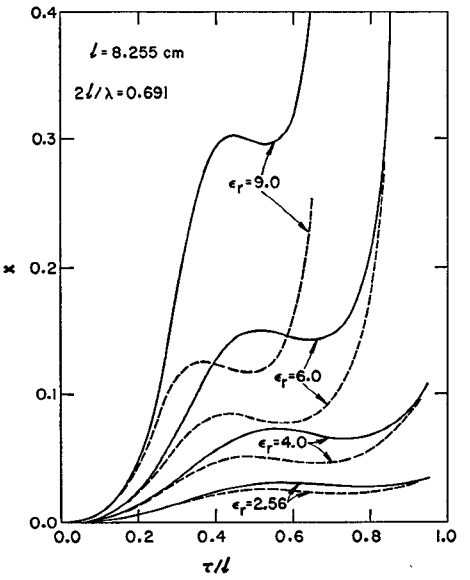

Fig. 3. Curves of $-x_1$ (dashed) and x_2 (solid) versus τ/l for empty to side-slab-filled waveguide junction [geometry of Fig. 1(a)].

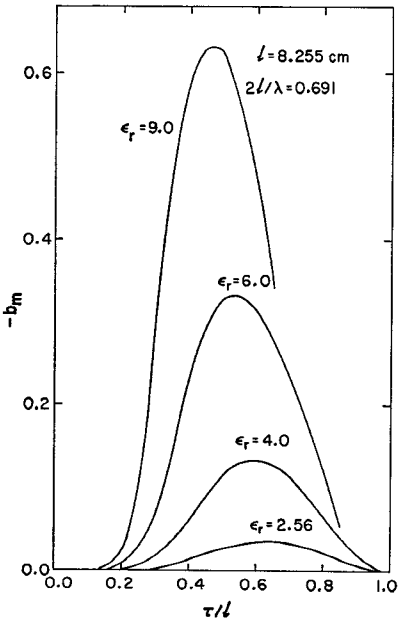

Fig. 4. Curves of b_m versus τ/l for an empty to side-slab-filled waveguide junction.

out by using the Crout method and was written by B. S. Garbor of the Argonne National Laboratory. Both the series impedances Z_{S1} and Z_{S2} and the shunt admittance Y_m are found to be imaginary and converge to certain limits. Their values obtained from the 20- and 21-term approximations agree to better than 10^{-5}. These impedances and the admittance were normalized to the characteristic wave impedance of the empty waveguide with the same dimensions at the same frequency, and are presented as $-jx_1$, jx_2, and $-jb_m$ in the figures throughout this paper.

Computations of the effect of the dielectric thickness on the normalized characteristic wave impedance $z_0[\equiv Z_0/Z_0$ (empty guide)] of the partially filled waveguides are presented

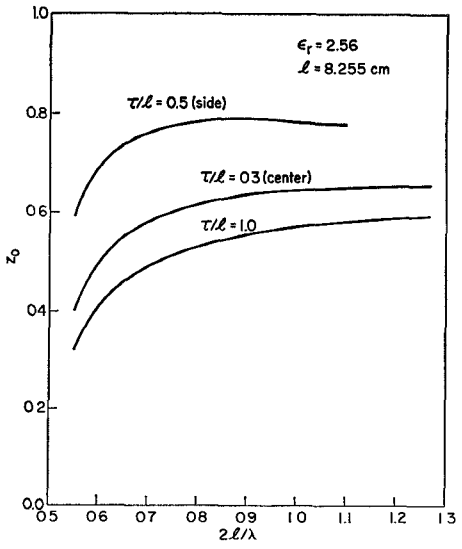

Fig. 5. Normalized characteristic wave impedance z_0 versus normalized frequency ($2l/\lambda$) curves for 1) side-slab-filled waveguide with $\tau/l = 0.5$, 2) center-slab-filled waveguide with $\tau/l = 0.3$, and 3) completely filled waveguide. The dielectrics employed are Rexolite.

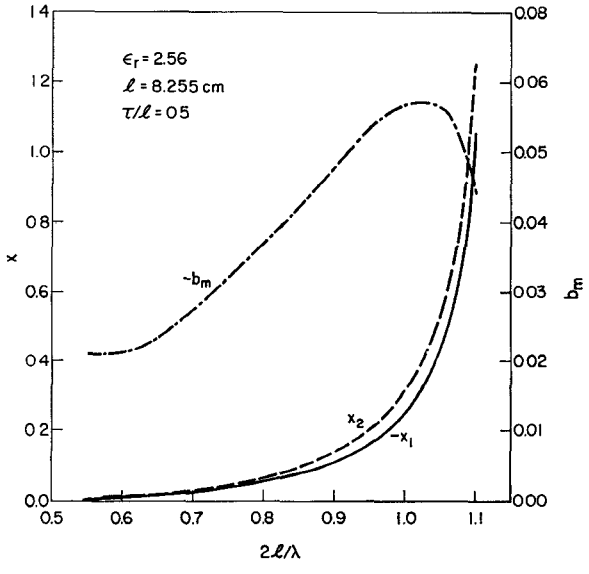

Fig. 6. Typical curves of x_1, x_2, and b_m versus $2l/\lambda$ for a junction shown in Fig. 1(a). Note the rapid increases of x_1 and x_2 just below the cutoff of TE_{03} mode of the partially dielectric-filled waveguide near $2l/\lambda = 1.1$.

in Fig. 2 for Rexolite ($\epsilon_r = 2.56$), quartz ($\epsilon_r = 4.0$), beryllia ($\epsilon_r = 6\,0$), and alumina ($\epsilon_r = 9.0$) at 1.255 GHz ($2l/\lambda = 0.691$). With $z_1 = z_0$ (of Fig. 2) and $z_2 \equiv 1$, the reflection due to the ideal transformer in Fig. 1(g) is specified. The corresponding x_1, x_2, and b_m curves for these dielectrics are presented in Figs. 3 and 4.

The effect of changing operating frequency for a given waveguide junction is presented in Figs. 5 and 6 for Rexolite. The top curve in Fig. 5 [labeled $\tau/l = 0.5$ (side)] shows that z_0 for the partially dielectric-filled waveguide increases, reaching a maximum value near $2l/\lambda \approx 0.9$, and drops off slightly thereafter as the frequency is increased [$f(\equiv c/\lambda)$ is represented by a dimensionless variable $2l/\lambda$]. The equivalent

TABLE I

	f(GHz)	ρ_{meas}	ρ_{cal} exact	ρ_{cal} approx.	d/d_L
Rexolite slabs $\epsilon_r = 2.56$ $\tau/l = 0.5796$	1.255	1.40	1.446	1.450	3.15
Alumina slabs $\epsilon_r = 8.2$ $\tau/l = 0.2773$	2.4	1.72	1.629	1.643	5.19
	2.6	1.52	1.504	1.527	3.91
	2.8	1.50	1.452	1.496	3.07
	3.0	1.59	1.417	1.505	2.43
	3.2	1.68	1.370	1.540	1.87

graphs for other dielectrics are similar to those of Figs. 5 and 6 and are not presented.

From these graphs one concludes the following.

1) The junction-reactance network causes no reflection when the field distribution functions of the two waveguides across a junction become identical (see the region at $\tau/l \approx 0.0$ and 1.0 in Figs. 3 and 4). However, reflection would still occur due to the difference between z_1 and z_2.

2) The series reactance at the side of the more heavily loaded waveguide is capacitive, the series reactance at the side of less heavily loaded waveguides is inductive, and the shunt admittance is inductive and is normally the major contributor to reflection among the three elements of the junction-reactance network [see Fig. 1(g)].

3) As the dielectric constant ϵ_r of the slabs increases, x_1, x_2, and b_m become larger (see Figs. 3 and 4) and the normalized characteristic wave impedance z_1 of the more heavily loaded waveguide decreases (see Fig. 2). Thus the reflection due to the waveguide junction is also increased.

4) The series reactances x_1 and x_2 increase rapidly as the operating frequency approaches the cutoff of the next higher order mode (TE_{03} mode for our case) of the more heavily loaded waveguide. Thus despite the small dielectric constant in the slabs, the reflection due to the junction-reactance network can still be considerable at the region immediately below the cutoff of the TE_{03} mode of the more heavily loaded waveguide.

5) Above the cutoff of TE_{03} mode of the more heavily loaded waveguide, where both TE_{01} and TE_{03} modes may propagate (see regions of $\tau/l > 0.85$ for $\epsilon_r = 6.0$ curves and $\tau/l > 0.65$ for $\epsilon_r = 9.0$ curves in Figs. 3 and 4, or regions of $2l/\lambda > 1.1$ in Fig. 6), the two-port network representations is no longer valid. No values of x_1, x_2, and b_m in these regions are given.

VI. Experimental Measurements

To verify the above calculation experimentally, a slotted waveguide was first connected to a matched source and terminated into a matched load (with VSWR < 1.03). Two identical Rexolite slabs were fabricated and placed at the two sides of the slotted waveguide. The semi-infiite geometry of Fig. 1(a) was simulated by matching the partially dielectric-filled waveguide to the source using a partially dielectric-filled impedance transformer [16]. Measurements were also carried out at S-band frequencies for alumina slab loading to observe the effect of larger ϵ_r. The measured VSWR, ρ_{meas}, is tabulated in Table I. Also tabulated in Table I are two columns of calculated VSWR, ρ_{cal}. The first of these was obtained by using the

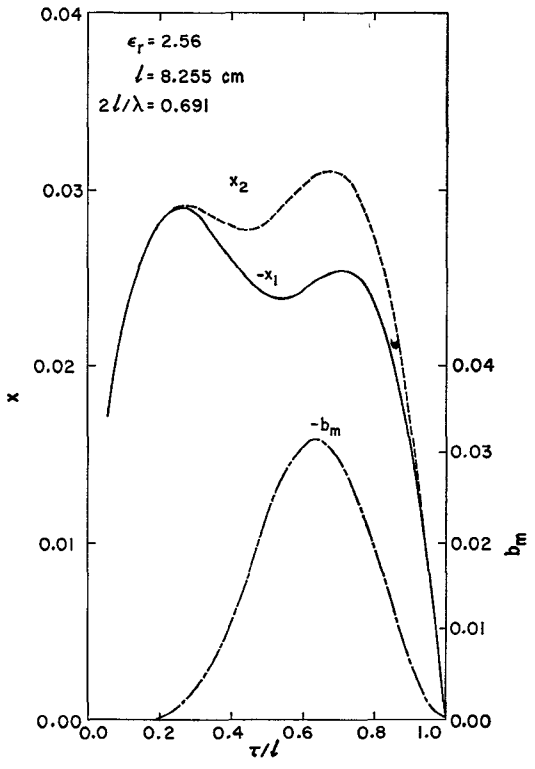

Fig. 7. Curves of x_1, x_2, and b_m versus τ/l for a completely filled to side-slab-filled waveguide junction [see Fig. 1(b)] with $\epsilon_r = 2.56$.

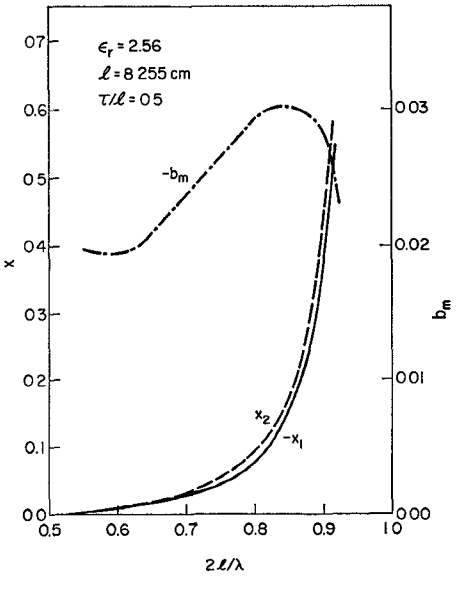

Fig. 8. Typical curves of x_1, x_2, and b_m versus $2l/\lambda$ for a completely filled to side-slab-filled waveguide junction. Note the rapid increases of x_1 and x_2 near $2l/\lambda \approx 0.9$, which is just below the cutoff of TE_{03} mode of the completely filled waveguide.

full equivalent circuit of Fig. 1(g). The second column is an approximate calculation with the effect of junction reactances neglected. Agreements between ρ_{meas} and ρ_{cal} are good. Deviations of ρ_{meas} from the exact calculation of ρ_{cal} occur only toward the higher frequency end, where the attenuation length d_L of the lowest evanescent mode in the transformer

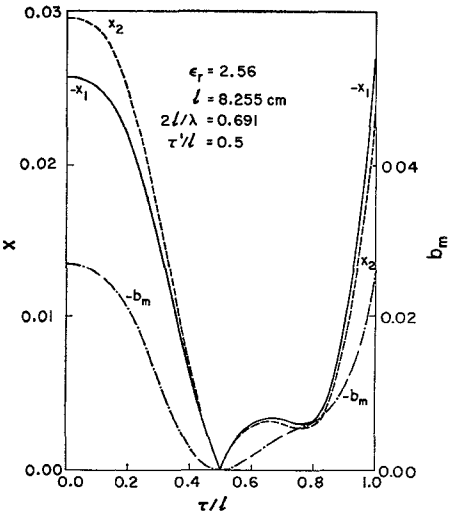

Fig. 9. Typical curves of x_1, x_2, and b_m with τ/l for a junction between two side-slab-filled waveguides [see Fig. 1(c)] with $\epsilon_r = 2.56$. The slab thickness in one waveguide is fixed at $\tau'/l = 0.5$. Note that the signs of the series reactances change at $\tau/l = 0.5$, where the second waveguide becomes more heavily loaded than the first one.

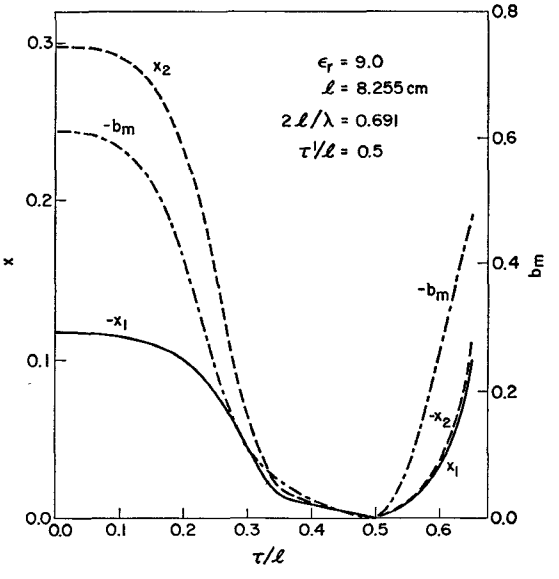

Fig. 10. Curves of x_1, x_2, and b_m versus τ/l for a junction between two side-slab-filled waveguides with $\epsilon_r = 9.0$. Note that the junction parameters are large for materials with large dielectric constants.

section becomes comparable to the length d of the transformer, and the input matching transformers employed in these measurements become less effective. The ratios of d/d_L are listed in the last column as references. Comparisons between the exact and approximate calculations in Table I also show that most of the reflections from the above junctions come from the ideal transformer, and the inclusion of the junction reactances in our calculation tends to reduce the reflection from that of an ideal transformer.

VII. Extension Into Other Kinds of Rectangular-Waveguide Junctions

The modal-expansion matrix-inversion method of the previous section can be readily applied to several different

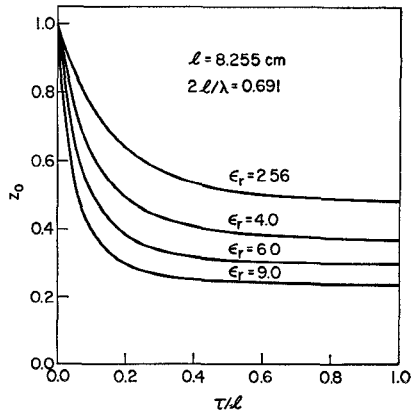

Fig. 11. Normalized characteristic wave impedance z_0 of the center-slab-filled waveguide [the partially dielectric-filled ones in Fig. 1(d)–(f)] versus normalized dielectric thickness τ/l for different dielectrics.

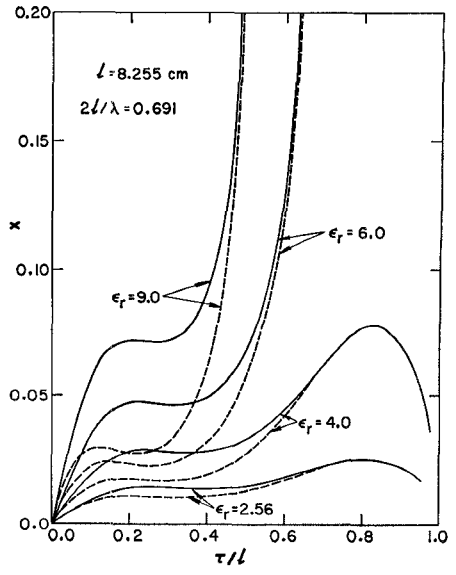

Fig. 12. Curves of $-x_1$ (dashed) and x_2 (solid) versus τ/l for an empty to center-slab-filled waveguide junction [see Fig. 1(d)].

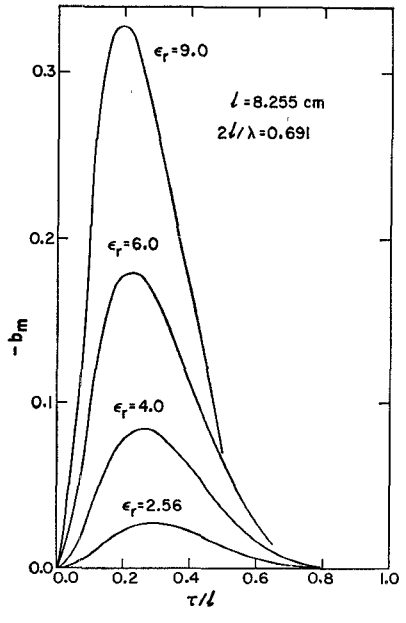

Fig. 13. Curves of b_m versus τ/l for an empty to center-slab-filled waveguide junction. Note that the peak of b_m is at $\tau/l \approx 0.3$ (compare to Fig. 4).

junctions. They are shown in Fig. 1(b)–(f). For these new geometries, the field-distribution functions $f_m(y)$ and $g_n(y)$ are replaced by the appropriate field-distribution functions [$F_m(y)$ for the partially dielectric-filled waveguide, and cosine functions for empty or completely filled waveguides]. Several of these functions, together with their respective dispersion relations, are presented in the Appendix. The corresponding $\Lambda_m^{(1)}$ and p_{mn} are also defined by (10) and (20). For geometry shown in Fig. 1(b), the characteristic impedances z_1 and z_2 of the two waveguides are give by the well-known formula for the filled waveguide or by the z_0 curves in Fig. 2 for partially filled waveguides. The parameters x_1, x_2, and b_m for the completely filled to partially filled junctions [Fig. 1(b)] with $\epsilon_r = 2.56$ are given in Fig. 7 for different thicknesses τ/l and in Fig. 8 for changing frequency.

Similar graphs of x_1, x_2, and b_m versus τ/l for the junction with the geometry of Fig. 1(c) are shown in Figs. 9 and 10. In these figures, $\tau'/l = 0.5$ is chosen in one waveguide so that x_1, x_2, and b_m are maximized when the second waveguide is either empty or completely filled with dielectrics (i.e., $\tau/l = 0$ or 1). Note that the reflection due to a junction with large dielectric step (i.e., large $|\tau' - \tau|/l$) can be greatly reduced by replacing it with several junctions, which are separated approximately by a quarter wavelength and have smaller dielectric steps. The method for impedance matching using partially dielectric-filled waveguides is presented elsewhere [16].

Other waveguide junctions involving center-slab-filled waveguides [shown in Fig. 1(d)–(f)] were also investigated. In these waveguides, slabs are placed at locations where E_x and H_y due to the propagating (TE_{01}) mode are high. The loading due to the thin slabs in these waveguides becomes more effective, and the characteristic wave impedances of them (shown in Fig. 11) drop off rapidly at small τ/l (compare Fig. 11 to Fig. 2). A typical curve of z_0 versus $2l/\lambda$ for a center-slab-filled waveguide is also given in Fig. 5 [labeled $\tau/l = 0.3$ (center)]. The effects of dielectric thickness (τ/l) and frequency ($2l/\lambda$) on x_1, x_2, and b_m are given in Figs. 12–18. Careful examination of these figures shows that despite their differences, the five-point conclusion given in Section V can still be applied to junctions given in Fig. 1(b)–(f). Moving the side slabs to the center of the waveguide also causes the peaks of b_m curves to shift from $\tau/l \approx 0.5$ to $\tau/l \approx 0.3$.

VIII. Conclusion

The partially dielectric-filled waveguide junctions have been investigated, and the results were presented in the form of parameters of the equivalent circuit. Effects of different dielectric constant ϵ_r, dielectric thickness τ, operating frequency f, and the physical location of the dielectric slabs (geometry) on these parameters were studied and presented in graphs. Several general characteristics are found to be applied to all six geometries and are presented in Section V. With

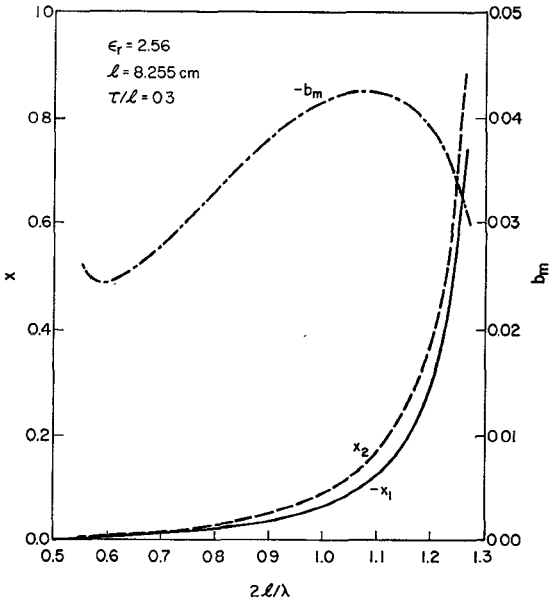

Fig. 14. Typical curves of x_1, x_2, and b_m versus $2l/\lambda$ for an empty to center-slab-filled waveguide junction.

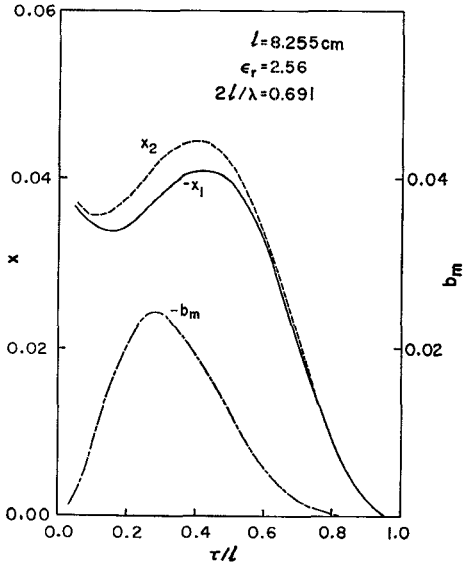

Fig. 15. Curves of x_1, x_2, and b_m versus τ/l for a completely filled to center-slab-filled waveguide junction [see Fig. 1(e)] with $\epsilon_r = 2.56$.

these basic understandings, an impedance-matching technique for partially dielectric-filled waveguide systems can be easily developed. Since the modal-expansion matrix-inversion method is general in nature, it is expected to apply to other types of partially dielectric-filled junctions as well.

Appendix

Field-Distribution Functions and Dispersions of the Partially Dielectric-Filled Waveguides

1) With dielectric slabs at the sides and real γ_m, the field distribution function and dispersion are given by (4) and (7).

2) With dielectric slabs at the sides and imaginary $\gamma_m (\equiv j\gamma_m')$

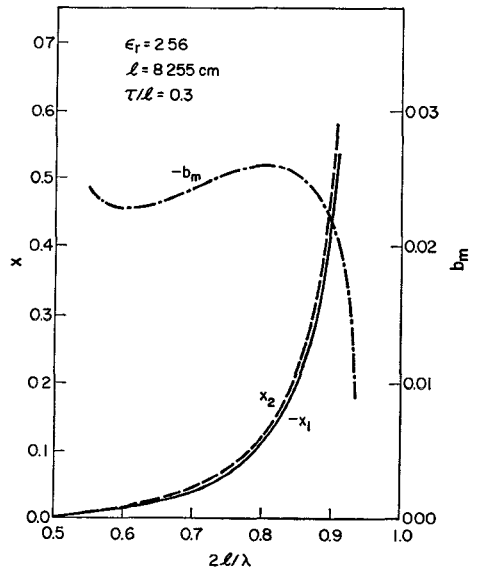

Fig. 16. Typical cuves of x_1, x_2, and b_m versus $2l/\lambda$ for a completely filled to center-slab-filled waveguide junction.

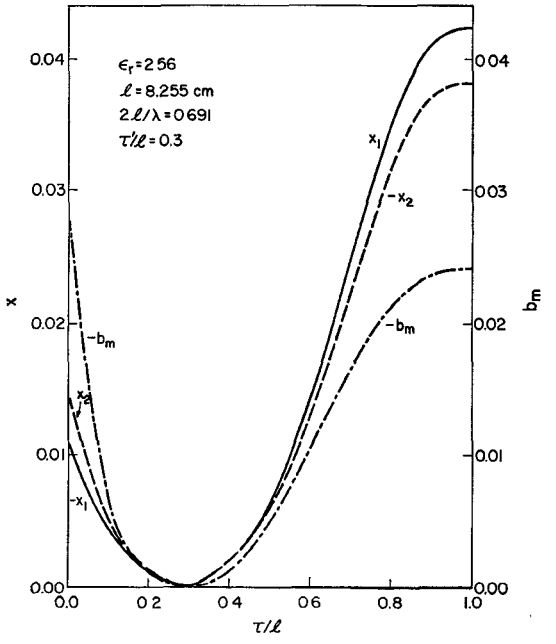

Fig. 17. Curves of x_1, x_2, and b_m versus τ/l for a junction between two center-slab-filled waveguide junctions [see Fig. 1(f)] with $\epsilon_r = 2.56$.

$$F_m(y) = \frac{1}{\sqrt{2\Lambda_m^{(1)}}} \cdot \begin{cases} \sin \alpha_m \tau \cosh \gamma_m' y, & 0 < |y| < l - \tau \\ \cosh \gamma_m'(l - \tau) \sin \alpha_m (l - |y|), & l - \tau < |y| < l \end{cases} \qquad m = 1, 3, \cdots \quad (29)$$

and

$$\gamma_m' \tanh \gamma_m'(l - \tau) = -\alpha_m \cot \alpha_m \tau. \quad (30)$$

3) With a dielectric slab at the center and real γ_m

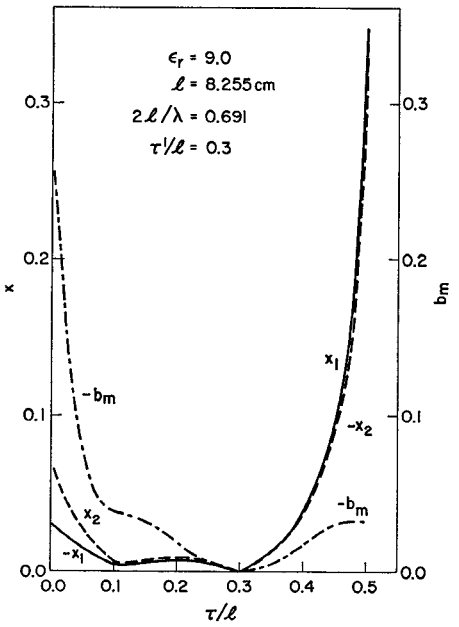

Fig. 18. Curves of x_1, x_2, and b_m versus τ/l for a junction between two center-slab-filled waveguide junctions with $\epsilon_r = 9.0$. The parameters are large at large $|\tau' - \tau|/l$ for this ϵ_r.

$$F_m(y) = \frac{1}{\sqrt{2\Lambda_m^{(1)}}} \cdot \begin{cases} \sin \gamma_m(l-\tau) \cos \alpha_m y, & 0 < |y| < \tau \\ \cos \alpha_m \tau \sin \gamma_m(l - |y|), & \tau < |y| < l \end{cases} \quad m = 1, 3, \cdots \tag{31}$$

and

$$\gamma_m \cot \gamma_m(l-\tau) = \alpha_m \tan \alpha_m \tau. \tag{32}$$

4) With a dielectric slab at the center and imaginary $\gamma_m (\equiv j\gamma_m')$

$$F_m(y) = \frac{1}{\sqrt{2\Lambda_m^{(1)}}} \cdot \begin{cases} \sinh \gamma_m'(l-\tau) \cos \alpha_m y, & 0 < |y| < \tau \\ \cos \alpha_m \tau \sinh \gamma_m'(l-y), & \tau < |y| < l \end{cases} \quad m = 1, 3, \cdots \tag{33}$$

and

$$\gamma_m' \coth \gamma_m'(l-\tau) = \alpha_m \tan \alpha_m \tau. \tag{34}$$

References

[1] L. Pincherle, "Electromagnetic waves in metal tubes filled longitudinally with two dielectrics," *Phys. Rev.*, vol. 66, pp. 118–130, Sept. 1944.

[2] C. G. Montgomery, R. H. Dicke, and E. M. Purcell, *Principles of Microwave Circuits* (M.I.T. Rad. Lab. Series), vol. 8. New York: McGraw-Hill, 1948, pp. 385–389.

[3] N. Marcuvitz, *Waveguide Handbook* (M.I.T. Rad Lab. Series), vol. 10. New York: McGraw-Hill, 1951, pp. 387–393.

[4] R. E. Collin, *Field Theory of Guided Waves*. New York: McGraw-Hill, 1960.

[5] R. F. Harrignton, *Time Harmonic Electromagnetic Fields*. New York: McGraw-Hill, 1961, p. 162.

[6] P. H. Vartanian, W. P. Ayres, and A. L. Helgesson, "Propagation in dielectric slab loaded rectangular waveguide," *IRE Trans. Microwave Theory Tech.*, vol. MTT-6, pp. 215–222, Apr. 1958.

[7] R. Seckelmann, "Propagation of TE modes in dielectric loaded waveguides," *IEEE Trans. Microwave Theory Tech.*, vol. MTT-14, pp. 518–527, Nov. 1966.

[8] N. Eberhardt, "Propagation in the off center E-plane dielectrically loaded waveguide," *IEEE Trans. Microwave Theory Tech.*, vol. MTT-15, pp. 282–289, May 1967.

[9] W. E. Hord and F. J. Rosenbaum, "Approximation technique for dielectric loaded waveguides," *IEEE Trans. Microwave Theory Tech.*, vol. MTT-16, pp. 228–233, Apr. 1968.

[10] F. E. Gardiol, "Higher-order modes in dielectrically loaded rectangular waveguides," *IEEE Trans. Microwave Theory Tech.*, vol. MTT-16, pp. 919–924, Nov. 1968.

[11] R. L. Kustom, C. T. M. Chang, and J. W. Dawson, "Propagating and transverse deflecting modes in a dielectric filled rectangular waveguide," Argonne Nat. Lab., Argonne, Ill., High Energy Facilities Div. Internal Rep. RLK/CTMC/JWD-1, Mar. 1, 1970.

[12] a) C. T. M. Chang, J. W. Dawson, and R. L. Kustom, "A dielectric loaded slow wave structure for separation of relativisitic particles," *IEEE Trans. Nucl. Sci.*, vol. NS-16, pp. 526–530, June 1969.
b) John W. Dawson and R. L. Kustom, "Traveling wave particle separation including a rectangular waveguide line with a dielectric material," U. S. Patent 3 609 351, Sept. 1971.

[13] G. F. Bland and A. G. Franco, "Phase-shift characteristics of dielectric loaded waveguide," *IRE Trans. Microwave Theory Tech. (1962 Symposium Issue)*, vol. MTT-10, pp. 492–496, Nov. 1962.

[14] G. N. Tsandoulas, D. H. Temme, and F. G. Willwerth, "Longitudinal section mode analysis of dielectrically loaded rectangular waveguides with application to phase shifter design," *IEEE. Trans. Microwave Theory Tech.*, vol. MTT-18, pp. 88–95, Feb. 1970.

[15] W. J. Ince and E. Stern, "Nonreciprocal remanence phase shifters in rectangular waveguide," *IEEE Trans. Microwave Theory Tech.*, vol. MTT-15, pp. 87–95, Feb. 1967.

[16] C. T. M. Chang, "Impedance matching using partially dielectric-filled waveguides," Argonne Nat. Lab., Argonne, Ill., High Energy Facilities Div. Internal Rep. CTMC-1, Nov. 1, 1972.

[17] R. E. Collin and J. Brown, "The calculation of the equivalent circuit of an axially unsymmetrical waveguide junction," *Proc. Inst. Elec. Eng.*, vol. 103, part C, pp. 121–128, Mar. 1956.

[18] C. M. Angulo, "Discontinuities in a rectangular waveguide partially filled with dielectric," *IRE Trans. Microwave Theory Tech.*, MTT-5, pp. 68–74, Jan. 1957.

[19] R. E. Collin and R. M. Vaillancourt, "Application of Rayleigh–Ritz method to dielectric steps in waveguides," *IRE Trans. Microwave Theory Tech.*, vol. MTT-5, pp. 177–184, July 1957.

[20] J. Schwinger, in *Discontinuities in Waveguides*, D. S. Saxon, Ed. New York: Gordon, Feb. 1945.

[21] R. L. Kustom, R. E. Fuja, and C. T. M. Chang, "The Argonne National Laboratory microwave discharge chamber project," in *Proc. 1972 Int. Conf. Streamer Chamber Technology*.

[22] E. L. Ginzton, *Microwave Measurements*. New York: McGraw-Hill, 1957, p. 327.